Synechocystis ferredoxin/ferredoxin-NADP$^+$-reductase/NADP$^+$ complex: Structural model obtained by NMR-restrained docking

P. Nuno Palma[a], Bernard Lagoutte[b], Ludwig Krippahl[a], José J.G. Moura[a], Françoise Guerlesquin[c,*]

[a] *REQUIMTE, Departamento de Química, Faculdade de Ciências e Tecnologia, Universidade Nova de Lisboa, 2859-516 Caparica, Portugal*
[b] *Service de Bioénergétique, URA 2096, CNRS, Département de Biologie Joliot Curie, CEA Saclay, 91191 Gif sur Yvette Cedex, France*
[c] *Unité de Bioénergétique et Ingénierie des Protéines, IBSM-CNRS, 31 chemin Joseph Aiguier, 13402 Marseille Cedex 20, France*

Received 16 May 2005; revised 27 June 2005; accepted 5 July 2005

Available online 8 August 2005

Edited by Miguel De la Rosa

Abstract Ferredoxin (Fd) and ferredoxin-NADP$^+$-reductase (FNR) are two terminal physiological partners of the photosynthetic electron transport chain. Based on a nuclear magnetic resonance (NMR)-restrained-docking approach, two alternative structural models of the Fd–FNR complex in the presence of NADP$^+$ are proposed. The protein docking simulations were performed with the software BiGGER. NMR titration revealed a 1:1 stoichiometry for the complex and allowed the mapping of the interacting residues at the surface of Fd. The NMR chemical shifts were encoded into distance constraints and used with theoretically calculated electronic coupling between the redox cofactors to propose experimentally validated docked complexes.

Keywords: Ferredoxin; Ferredoxin NADP$^+$-reductase; Complex; Docking and NMR

1. Introduction

Short-lived non-covalent complexes formed between electron-transfer proteins are essential for the function of energy conserving systems such as photosynthesis and respiration. The molecular recognition process involves sequential steps: formation of a transient complex, electron transfer, dissociation and diffusion. The active sites must come in close contact to produce an efficient electron-transfer device, being the specificity and the efficiency of the electron transfer dictated and controlled by the details of the non-covalent interactions. While the three-dimensional (3D) structures as well as a wealth of information are available for many redox proteins, very few structures of electron-transfer complexes have been solved to date. Due to the low affinity constants, it is difficult to obtain co-crystals of these transient complexes. However, two structures of the FNR/ferredoxin (Fd) complexes from *Z. Maize* and *Anabaena* PCC7119 have been solved by crystallography [1,2]. In order to give a model of the ternary NADP/FNR/Fd complex, we have used in the present paper a nuclear magnetic resonance (NMR)-restrained docking approach [3–5].

Ferredoxin-NADP$^+$-reductases (FNR) are flavine adenine dinucleotide (FAD) flavoproteins that catalyze the reduction of nicotinamide adenine dinucleotide phosphate (NADP$^+$) to NADPH during photosynthesis in plant, algae or cyanobacteria [6]. The electron transfer from photosystem I to FNR is mediated by a (2Fe–2S) Fd [7]. Fd is a small ubiquitous soluble protein involved in many cellular processes from prokaryotes to eukaryotes [8]. NMR allowed us to investigate the formation of a complex between FNR and Fd from *Synechocystis* sp. PCC 6803 (*Synechocystis*), in the presence or the absence of NADP. On the basis of sequence alignment (Fig. 1), a structural model of FNR has been obtained, and NMR-restrained docking enables us to propose two structural working models of the Fd/FNR/NADP$^+$ ternary complex.

2. Materials and methods

2.1. Expression and purification of the ^{15}N labeled Fd

The *petF* gene was PCR amplified, cloned and used for overexpression as previously reported [9]. The minimal medium (M9) was supplemented with ^{15}N ammonium sulfate (ISOTEC Inc., Matheson company, Miamisburg, USA). Purification of Fd was essentially as previously described [10] with an additional last step using hydrophobic chromatography (HiLoad phenyl Sepharose 16/10 from Pharmacia) eluted using a reverse gradient of ammonium sulfate (2.5–0 M) in 60 mM tricine buffer at pH 7.8. The final 422–276 OD ratio was of 0.55. Fd was equilibrated in 10 mM phosphate buffer and concentrated by ultrafiltration up to 4 mM as measured at 422 nm using an extinction coefficient of 9.68 $mM^{-1}\,cm^{-1}$.

2.2. Expression and purification of FNR

The plasmid encoding a truncated form of the *petH* gene was a gift of Dr. J. van Thor, modified in order to start translation at the codon 113 of the original gene [11]. Purification procedure of *Synechocystis* FNR followed a similar scheme as for Fd. Overexpressed FNR was precipitated between 55% and 70% ammonium sulfate saturation and solubilized in 20 mM tricine, pH 7.8. The protein sample first loaded on a Hitrap *Q* Sepharose HP column (Pharmacia) was further purified on a phenyl Sepharose matrix (HiLoad phenyl Sepharose 16/10 from Pharmacia) eluted by a reverse ammonium sulfate gradient (1.6–0 M in tricine 80 mM, pH 7.8). Pure FNR was eluted at 0.85 M salt. The 460–274 OD ratio after dialysis against 10 mM phosphate, pH 6.5, was 0.14. The protein concentration for NMR studies was estimated based on an extinction coefficient of 10.8 $mM^{-1}\,cm^{-1}$ at 460 nm.

*Corresponding author. Fax: +33 4 91 16 45 78.
E-mail address: guerlesq@ibsm.cnrs-mrs.fr (F. Guerlesquin).

Abbreviations: FAD, flavine adenine dinucleotide; Fd, ferredoxin; FNR, ferredoxin-NADP$^+$-reductase; HSQC, heteronuclear single quantum coherence; NADP$^+$, nicotinamide adenine dinucleotide phosphate; NMR, nuclear magnetic resonance; *Synechocystis*, *Synechocystis* sp. PCC 6803

0014-5793/$30.00
doi:10.1016/j.febslet.2005.07.027

A Ferredoxin-NADP$^+$ Reductase

```
Z.M.   ----PATAKAKKESKKQEEGVVTNLYKPKEPYVGRCLLNTKITGDDAPGETWHMVFS-TEGKIPYREGQSIGVIADGVDKNGKPHKVRLY
Syn.   ----------TPKEKKADDIPVNIYRPKTPYIGKVLENYPLVREGAIGTVQHLTFDLSAGDLRYLEGQSIGIIPPGEDDKGKPHKLRLY
Ana.   ----------TQAKAKHADVPVNLYRPNAPFIGKVISNEPLVKEGGIGIVQHIKFDLTGGNLKYIEGQSIGIIPPGVDKNGKPEKLRLY
                  ....|....|....|....|....|....|....|....|....|....|....|....|....|....|....|....
                  1        10        20        30        40        50        60        70

Z.M.   SIASSAIGDFGDSKTVSLCVKRLIYTN-DAGEIVKGVCSNFLCDLQPGDNVQITGPVGKEMLMPKDPNATIIMLATGTGIAPFRSFLWKM
Syn.   SIASTRHGDFGDDKTVSLCVRQLEYQN-EAGETVQGVCSTYLCNIKEGDDIAITGPVGKEMLLPPDEDANIVMLATGTGIAPFRAFLWRM
Ana.   SIASTRHGDDVDDKTISLCVRQLEYKHPESGETVYGVCSTYLTHIEPGSEVKITGPVGKEMLLPDDPEANVIMLATGTGIAPMRTYLWRM
       |....|....|....|....|....|....|....|....|....|....|....|....|....|....|....|....|....|....
       80        90        100       110       120       130       140       150       160

Z.M.   FFEKH----DDYKFNGLGWLFLGVPTSSSLLYKEEFGKMKERAPENFRVDYAVSREQTNAAGERMYIQTRMAEYKEELWELLKKDNTYVY
Syn.   FKEQH----EDYKFKGLAWLIFGIPKSENILYKDDLEKMAAEFPDNFRLTYAISREQQNAEGGRMYIQHRVAENAEELWNLMQNPKTHTY
Ana.   FKDAERAANPEYQFKGFSWLVFGVPTTPNILYKEELEEIQQKYPDNFRLTYAISREQKNPQGGRMYIQDRVAEHADELWQLIKNQKTHTY
       |....|....|....|....|....|....|....|....|....|....|....|....|....|....|....|....|....|....
       170       180       190       200       210       220       230       240       250

Z.M.   MCGLKGMEKGIDDIMVSLAEKDGIDWFDYKKQLKRGDQWNVEVY
Syn.   MCGLKGMEPGIDEAFTALAEQNGKEWTTFQREMKKEHRWHVETY
Ana.   ICGLRGMEEGIDAALSAAAAKEGVTWSDYQKDLKKAGRWHVETY
       |....|....|....|....|....|....|....|....|...
       260       270       280       290       300
```

B Ferredoxin

```
Z.M.   ATYNVKLI-TPEG-EVELQVPDDVYILDQAEEDGIDLPYSCRAGSCSSCAGKVVSGSVDQSDQSYLDDGQIADGWVLTCHAYPTSDVVI
Syn.   ASYTVKLI-TPDG-ESSIECSDDTYILDAAEEAGLDLPYSCRAGACSTCAGKITAGSVDQSDQSFLDDDQIEAGYVLTCVAYPTSDCTI
Ana.   ATFKVTLINEAEGTKHEIEVPDDEYILDAAEEQGYDLPFSCRAGACSTCAGKLVSGTVDQSDQSFLDDDQIEAGYVLTCVAYPTSDVVI
       ....|....|....|....|....|....|....|....|....|....|....|....|....|....|....|....|....|....
       1         10        20        30        40        50        60        70        80

Z.M.   ETHKEEELTGA
Syn.   ETHKEEDLY--
Ana.   QTHKEEDLY--
       |....|....|
       90        100
```

Fig. 1. Multiple sequence alignment for (A) FNRs and (B) Fds, from *Z. Maize* (*Z.M.*), *Synechocystis* (*Syn.*) and *Anabaena* (*Ana.*). Sequence numbering was taken from *Anabaena*. Residues mapped by NMR in *Maize* system [2] and in *Synechocystis* (this work), are displayed in double underline and bold. Multiple sequence alignment was performed with ClustalW.

2.3. Nuclear magnetic resonance

NMR experiments were carried out on a Bruker DRX500 spectrometer at 293 K. 2D ^1H–^{15}N heteronuclear single quantum coherence (HSQC) spectra were recorded using a watergate pulse sequence in the TPPI mode. The spectral widths are 2500 Hz for ^1H and 2027 Hz for ^{15}N. 1024 data points in t_2 and 64 transients for each 128 t_1 were used. The ^1H and ^{15}N chemical shifts of the free-Fd were found in agreement with those previously reported [12]. Two sets of NMR titration experiments were performed with Fd samples, respectively, at 0.05 and 0.1 mM concentrations, in 10 mM phosphate buffer, pH 6.5, 10% D_2O. Small amounts of either FNR or FNR–NADP$^+$ (1:1) complex (2 mM concentration) were added to the Fd sample to obtain 0.12, 0.25, 0.5, 1, 2 or 5 M equivalents to Fd concentration.

2.4. Modeling

The structure of *Synechocystis* FNR was obtained by homology modeling using the X-ray structure (as template) of the homologous protein from *Anabaena* (sequence homology between the two proteins is 65%). The sequences were aligned (Fig. 1A) with the program ClustalW (http://www.ebi.ac.uk/clustalw) and that of the target molecule was overlaid on the 3D structure of the template protein. The atomic coordinates of the highest resolution structure of *Anabaena* FNR (pdb:1QUE, 1.8 Å) were used to model *Synechocystis* FNR apo-protein. Since 1QUE lacks the structure of NADP$^+$, the atomic coordinates of the co-substrate were taken from the 3D structure of *Pea* FNR (pdb:1QFY) and merged into the final *Synechocystis* structure. Note that the residues of the co-substrate binding pocket are extremely conserved; of the 23 residues that make close contacts (<4 Å) with NADP$^+$ in the Pea FNR structure, 18 are conserved, 4 show conservative mutations and only the C-terminal Ser308 is substituted by a non-equivalent Tyrosine residue in *Synechocystis*. Therefore, it is fair to assume that the two proteins may stabilize the substrate in the same conformation. A coarse structure prediction was first performed at the Swiss-Model web server [13] and the final model was optimized by energy minimization with the MMFF94 force field, as implemented in the molecular modeling package Sybyl (Tripos Inc., 1699 South Hanley Rd., St., Louis, MO 63144, USA.).

A structure of *Synechocystis* Fd is available from NMR, but lacks well resolved coordinates around the region of the FeS cluster. Therefore, a new model of the Fd was generated by overlaying the amino acid sequence of the *Synechocystis* protein onto the X-ray structure of the homologous Fd from *Anabaena* (pdb:1QT9, 1.3 Å) (sequence homology is 70%, Fig. 1B), followed by structure refinement, as described above.

2.5. Docking

Molecular interaction simulations were performed using the protein-docking algorithm BiGGER v.1.0 [5,14], and the entire molecular surfaces were searched, therefore, assuming no prior knowledge of the interacting surface regions.

2.6. NMR filtering

The perturbations of NMR chemical shifts of Fd caused by the presence of FNR can be used to probe the amino acids more closely involved in the formation of the complex. Once assigned to specific amino acids, these chemical shift perturbations may be translated into distance constraints, assuming that a nucleus is affected if it is within an arbitrary distance of 8 Å from any atom of the other partner. Only those solutions that minimize the number of constraint violations are retained for subsequent analysis.

2.7. Electron tunneling pathway filtering

The first-order rate constant for electron transfer k_{et} between a donor and an acceptor at fixed distance and orientation may be generally described by Marcus theory [15]. In the case of the electron-transfer reaction between the redox centers of two interacting proteins, k_{et} depends essentially on temperature, ΔG^0 (determined by the difference in redox potentials), the reorganization energy and the electronic coupling between the two redox centers. This last parameter is approximated by a decay function which is influenced by the distance and nature of the intervening medium, i.e., the nature of the putative electron-transfer pathway. For the purpose of comparing alternative binding orientations between two proteins, the first three contribution terms of k_{et} may be considered approximately constant and therefore, the structures presenting higher electronic coupling values should also allow for faster electron-transfer rates.

3. Results and discussion

3.1. NMR titration

^{15}N–^{1}H HSQC experiments carried out on ^{15}N labeled Fd in the presence of FNR alone or $NADP^+$-bound FNR revealed identical modifications of 12 resonances of the Fd. Among the 76 assigned residues of the Fd [12], 7 residues (L25, L35, R40, G49, L64, H90 and K91) were found substantially affected during the complex formation, in both cases (Fig. 2A). These resonances, corresponding to residues close to the FeS center of the Fd, are broaden in the spectrum of the free-Fd and progressively disappeared during the complex formation with FNR. However, the shifts of theses resonances, still observable at low FNR concentrations indicate that the corresponding amino acids are at the interacting site and that the complex is in fast exchange at the NMR time scale. Five other resonances, assigned to residues D26, G32, Y80, D84 and Y96, shifting more than 0.2 ppm for ^{15}N during the complex formation (Fig. 2B), were also selected. These 12 residues fairly dispersed through the Fd surface that surrounds the FeS center were used to define distance constraints to filter the docking results.

As attested by the saturation curves obtained from the Y96 chemical shift variations (Fig. 2C), the stoichiometry of the Fd/FNR and Fd/FNR–$NADP^+$ complexes was found to be 1:1. This stoichiometry is in agreement with gel filtration experiments (data not shown and [16]). The titration curves show that the affinity of the two proteins is slightly increased by the presence of $NADP^+$ (Fig. 2C). For this reason, we have investigated the docking of the two proteins in the presence of $NADP^+$.

3.2. Docking experiments

It is now generally assumed that transient complexes such as the ones formed between electron-transfer proteins have typically low association constants and are driven by long-range electrostatic interactions that favor the dynamic nature of their formation and dissociation. Due to the particular nature of such interaction, reliable docking simulations of electron-transfer complexes are more difficult to accomplish using general purpose docking algorithms. Instead, we have previously developed a successfully constrained docking hybrid methodology [3–5], which enriches the docking search space with solutions that are compatible with experimental evidence.

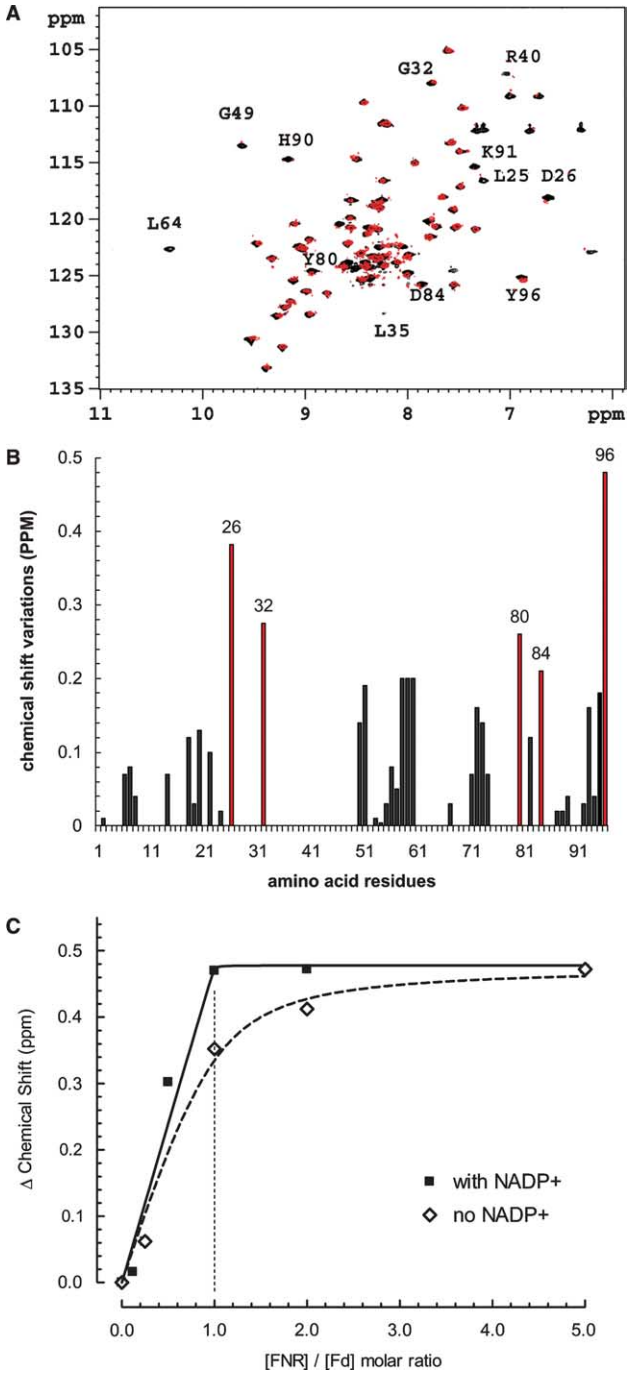

Fig. 2. (A) ^{15}N–^{1}H HSQC spectra of ^{15}N labeled Fd from *Synechocystis* in the absence of FNR (in black), and in the presence of NADP-bound FNR at a 1:0.5 Fd/FNR ratio (in red). The NMR experiments were recorded with a 500 MHz NMR spectrometer, at 293 K. The Fd concentration was 50 μM in 10 mM phosphate buffer, pH 6.5. The labeled residues were used for NMR-restrained docking. (B) Chemical shift variations observed in ^{15}N HSQC of *Synechocystis* Fd in the presence of *Synechocystis* FNR/$NADP^+$ complex at a stoichiometry of 1 Fd:0.5 FNR/$NADP^+$. (C) Titration curve of the *Synechocystis* Fd/FNR complex formation. Y96, ^{15}N resonance was followed during the titration: in the absence of $NADP^+$ (white diamonds), and in the presence of $NADP^+$ (black boxes). The curves represent best fits of data points with binding isotherms of 1:1 interactions.

The present docking experiment was performed using *Synechocystis* FNR/$NADP^+$ and Fd model structures described in Section 2. BiGGER protein docking algorithm was used

to generate and rank 5000 hypothetical docked structures, based on geometric surface complementarity and empirically based inter-residue affinity terms [5,14]. After a filtering step using NMR derived distance constraints, none of 5000 hypothetical docked structures fulfilled these 12 constraints. Indeed, D84 of Fd, whose ^{15}N resonance shifts about 0.2 ppm during complex formation, is located at the surface of Fd but, in contrast with all other selected residues, seats at the opposite side of the protein, relative to the FeS cluster. Therefore, it is not physically possible to have all marked residues simultaneously within 8 Å from the FNR partner and the target complex should be sought amongst the ones that minimize the number of NMR constraint violations. Seven hypothetical docked complexes fulfill 11 NMR constraints imposed and Fig. 3A represents their geometrical distribution. All seven complexes possess approximately the same interacting surface patches, with FAD and FeS cofactors separated by no more than 7.8 Å (between the C8M atom of isoalloxazine and the closest Iron atom). These models differ by varying degrees of rotation and translation along the inter-molecular axis.

To discriminate between those putative solutions, the initial 5000 docked structures were also evaluated for the theoretical electronic coupling constants, calculated between the corresponding redox cofactors (Section 2). The 50 top-scoring complexes which present the shortest electron tunneling pathlengths, were selected (Fig. 3B). As can be observed in Fig. 3, the NMR- and the electron tunneling-filtered docked solutions roughly share the same interacting regions. Three models are thus selected when applying simultaneously the two filters (Fig. 4A). Two of the three structures are very similar to each other (RMS deviation between α-carbons is 0.96 Å) and represent virtually the same solution.

From the results above, we were able to propose two alternative working models of the *Synechocystis* Fd/FNR/NADP$^+$ complex (Fig. 4B, models 1 and 2), which equally fulfill both experimental and theoretical constraints. The interaction scores computed with BiGGER algorithm are also very similar for the two structures. However, our current experimental or theoretical knowledge of this complex does not allow us to conclude which of them is more likely to represent the native complex.

3.3. Analysis of the structural models of Synechocystis Fd/FNR/NADP complex

The two models of the complex differ from each other by 3.7 Å RMSD (α-carbons), resulting from a slight rotation of the Fd molecule and a translation of around 6.5 Å along the surface of FNR. They share 19 common residues at the surface of Fd and only 11 on FNR, but interestingly, the molecular interfaces of the two model complexes show very similar percentages of non-polar atoms (about 60% in Fd and FNR). Model 1 is stabilized by three intermolecular salt-bridges (residues D11, D60 and E92 from Fd with K75, K264 and K77 from FNR, respectively) and three potential hydrogen bonds, involving S38, R40 and T46 from Fd, besides several hydrophobic contacts. Interactions in model 2 are less numerous with salt bridges and hydrogen bonds only between E29, G32 and E92 from Fd and K80, K77 and R21, respectively, from FNR. The interface areas

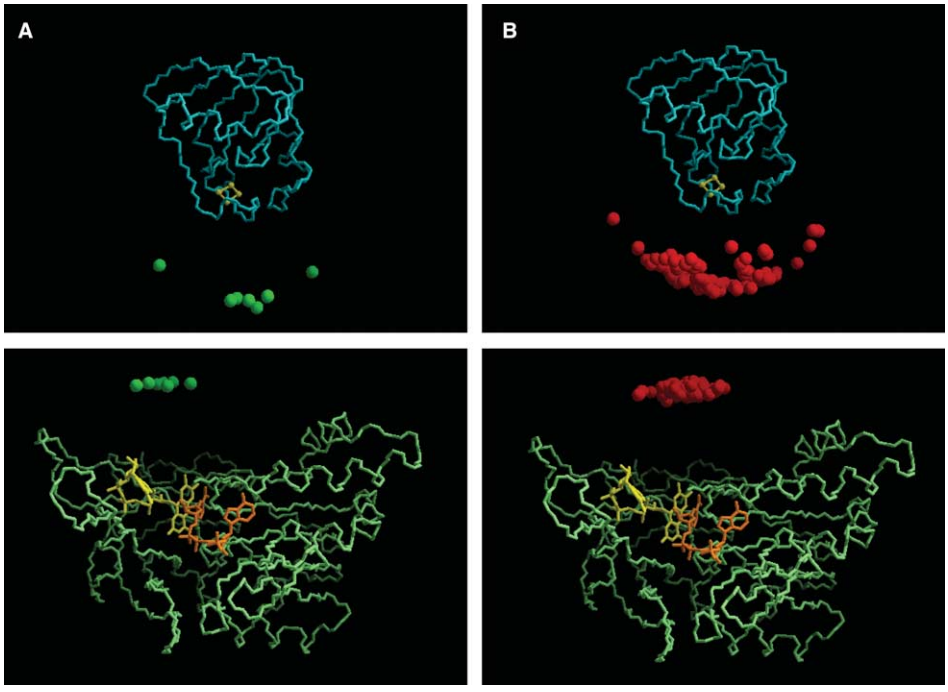

Fig. 3. Docking of the Fd/FNR/NADP$^+$ complex from *Synechocystis*. The top panels show the hypothetical docked positions of FNR (represented each by a small sphere located at its geometric center), relative to the structure of Fd (shown as blue backbone trace). The bottom panels represent the complementary view, i.e., the backbone of FNR is explicitly displayed in green and the position of the geometric center of each docked Fd molecule is represented with a sphere. FAD and NADP molecules are also shown in yellow and orange, respectively. Panel A: Filtered solutions (green) based on 12 distance constraints from NMR titrations (7 alternative poses). Panel B: Top 50 solutions (red) with minimal electron-transfer pathlengths between FeS and the isoalloxazine ring of FAD.

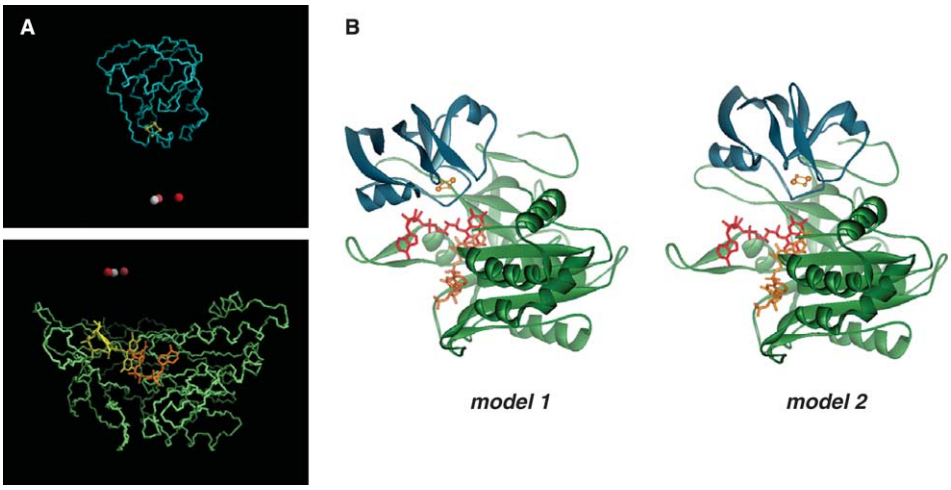

Fig. 4. Two hypothetical models of the Fd/FNR/NADP complex from *Synechocystis*. Panel A: Combined (intersection) set of docked solutions that fulfill all criteria simultaneously, color-coded according the BiGGER scoring function (red: higher, white: lower). Panel B: ''Best models'' of the complex FNR/Fd from *Synechocystis*.

of models 1 and 2 are 1530 and 2030 $Å^2$, respectively, which are within the most common range of 1600 ± 400 $Å^2$ for protein–protein complexes [17]. These values also compare well with the observed interface area (1600 $Å^2$) of the crystallographic 1:1 FNR/Fd complex from *Z. Maize* (pdb 1GAQ), even though the two models differ from that structure by as much as 8.0 and 8.6 Å RMSD, respectively. The interfaces of the two models are fairly compact, possessing a slightly smaller gap volume than that observed for the *Z. Maize* complex (7100 $Å^3$ versus 7800 $Å^3$). The crystallographic structure of the *Anabaena* complex shows, on the other hand, different characteristics. For comparison, the RMSD (α-carbon) between *Anabaena* complex and *Z. Maize* complex or *Synechocystis* models 1 and 2 are 7.5, 4.0 and 4.7 Å, respectively. The apparent heterogeneity of binding modes between Fd and FNR from different species may be a consequence of the low affinity of these transient complexes, mostly optimized for an efficient electron-transfer turnover. These data are in agreement with the NMR mapping of the *Maize* Fd interacting site [2] which is significantly different of that we found for *Synechocystis* system (Fig. 1).

A detailed analysis of the electron-transfer site shows that in both *Synechocystis* models, the two cofactors and $NADP^+$ substrate are in close proximity: the FeS–FAD distance is approximately 6.0 Å, and the FAD–$NADP^+$ distance is 2.3 Å. As represented in Fig. 5, these models suggest that Fd C39 has an essential role in electron transfer. C39 is one of the ligands of the FeS center and is positioned at the complex interface, inaccessible to water molecules and at 3.8 or 3.4 Å distance from the FAD (in models 1 or 2, respectively). The cysteine side chain therefore provides a potential bridge for the electron transfer, between the redox centers of the two proteins. In a similar way, it was proposed that C44 of *Maize* Fd is involved in a direct electron transfer through space between the prosthetic groups [2]. The involvement of C39 in *Synechocystis* complex or C44 in the *Maize* complex is certainly due to the different orientations of the two molecules in the complexes. In the current models of *Synechocystis* complex, like it was described in the crystallographic structure of *Maize* complex [2], the aromatic residue F63 of Fd, as well as Y37 are found at the interface, bordering the solvent excluded interface patch. However, their distances to the FeS cluster or the FAD group are higher than the FeS–FAD linear distance. It is therefore difficult to rationalize that these aromatic residues would provide a more efficient electron-transfer pathway than the direct through-bond pathway provided by C39. Indeed,

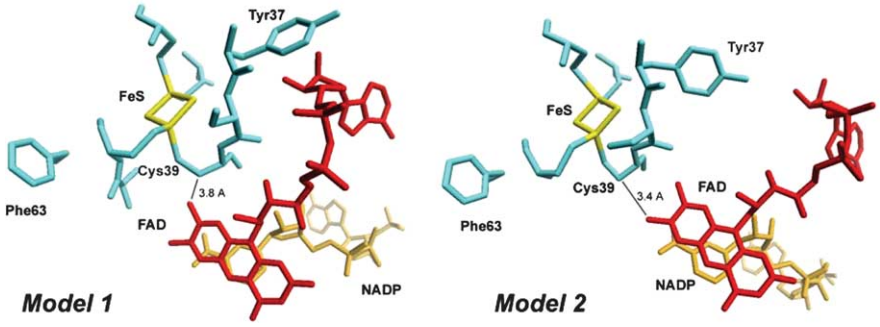

Fig. 5. Detailed view of the electron-transfer site in the two hypothetical models of $NADP^+$/FNR/Fd complex from *Synechocystis*. Fd's residues are colored in cyan, $NADP^+$ is in orange and FeS and FAD are in yellow.

$NADP^+$ is relatively buried inside FNR and the structural models suggest the absence of direct interactions between Fd and $NADP^+$.

Acknowledgments: The authors thank Michel Frey for helpful discussion on *Anabaena* FNR/Fd system. This work was supported by Fundação para a Ciência e Tecnologia, the French Embassy and ICCTI (no. 316C2) and the PICS program from CNRS and ICCTI (no. 1392). The starting pET vector for over-expression of the truncated *petH* gene was a kind gift of Dr. J. van Thor.

References

[1] Morales, R., Kachalova, G., Vellieux, F., Charon, M.H. and Frey, M. (2000) Crystallographic studies of the interaction between the ferredoxin-$NADP^+$ reductase and ferredoxin from the cyanobacterium *Anabaena*: looking for the elusive ferredoxin molecule. Acta Crystallogr. D: Biol. Crystallogr. 56, 1408–1412.

[2] Kurisu, G., Kusunoki, M., Katoh, E., Yamazaki, T., Teshima, K., Onda, Y., Kimata-Ariga, Y. and Hase, T. (2001) Structure of the electron transfer complex between ferredoxin and ferredoxin-NADP(+) reductase. Nat. Struct. Biol. 8, 117–121.

[3] Morelli, X., Czjzek, M., Hatchikian, C., Bornet, O., Fontecilla, J., Palma, P.N., Moura, J.J.G. and Guerlesquin, F. (2000) Structural model of the Fe-hydrogenase/cytochrome c_{553} complex combining transverse relaxation-optimized spectroscopy experiments and soft docking calculations. J. Biol. Chem. 275, 23204–23210.

[4] Morelli, X., Dolla, A., Czjzek, M., Palma, P.N., Blasco, F., Krippahl, L., Moura, J.J.G. and Guerlesquin, F. (2000) Heteronuclear NMR and soft docking: an experimental approach for a structural model of the cytochrome c_{553}–ferredoxin complex. Biochemistry 39, 2530–2537.

[5] Krippahl, L., Moura, J.J.G. and Palma, P.N. (2003) Modeling protein complexes with BiGGER. Proteins Struct. Funct. Genet. 52, 19–23.

[6] Carrillo, N. and Ceccarelli, E.A. (2003) Open questions in ferredoxin-$NADP^+$ reductase catalytic mechanism. Eur. J. Biochem. 270, 1900–1915.

[7] Shin, M. and Arnon, D.I. (1965) Enzymic mechanisms of pyridine nucleotide reduction of chloroplasts. J. Biol. Chem. 240, 1405–1411.

[8] Knaff, D.B. and Hirasawa, M. (1991) Ferredoxin-dependent chloroplast enzymes. Biochim. Biophys. Acta 1056, 93–125.

[9] Lagoutte, B., Hanley, J. and Bottin, H. (2001) Multiple functions for the C terminus of the PsaD subunit in the cyanobacterial photosystem I complex. Plant Physiol. 126, 307–316.

[10] Bottin, H. and Lagoutte, B. (1992) Ferredoxin and flavodoxin from the cyanobacterium *Synechocystis* sp. PCC 6803. Biochim. Biophys. Acta. 1101, 48–56.

[11] van Thor, J.J., Geerlings, T.H., Matthijs, H.C.P. and Hellingwerf, K.J. (1999) Kinetic evidence for the PsaE-dependent transient ternary complex photosystem I/ferredoxin/ferredoxin:NADP(+) reductase in a cyanobacterium. Biochemistry 38, 12735–12746.

[12] Lelong, C., Setif, P., Bottin, H., Andre, F. and Neumann, J.M. (1995) ^1H and ^{15}N NMR sequential assignment, secondary structure, and tertiary fold of [2Fe–2S] ferredoxin from *Synechocystis* sp. PCC 6803. Biochemistry 3, 14462–14473.

[13] Guex, N. and Peitsch, M.C. (1997) An environment for comparative protein modeling. Electrophoresis 18, 2714–2723.

[14] Palma, P.N., Krippahl, L., Wampler, J.E. and Moura, J.J.G. (2000) A new (soft) docking algorithm for predicting protein interactions. Proteins Struct. Funct. Genet. 39, 372–384.

[15] Marcus, R.A. and Sutin, N. (1985) Electron transfers in chemistry and biology. Biochim. Biophys. Acta 811, 265–322.

[16] Akashi, T., Matsumura, T., Ideguchi, T., Iwakiri, K., Kawakatsu, T., Taniguchi, I. and Hase, T. (1999) Comparison of the electrostatic binding sites on the surface of ferredoxin for two ferredoxin-dependent enzymes, ferredoxin-NADP(+) reductase and sulfite reductase. J. Biol. Chem. 274, 29399–29405.

[17] Lo Conte, L., Chothia, C. and Janin, J. (1999) The atomic structure of protein–protein recognition sites. J. Mol. Biol. 285, 2177–2198.